Optimal Wavelet for Single- and Multi-frequency Signals

A. Fedoseyev,[1, a)] J.-J. Malosse,[1, b)] and S. Tsynkov[2, c)]

[1]*Ultra Quantum Inc., Huntsville, Alabama, USA*
[2]*North Carolina State Univercity,Raleigh,North Carolina, USA*

[a)]Corresponding author: af@ultraquantum.com
[b)]jjm@ultraquantum.com
[c)]tsynkov@math.ncsu.edu

Abstract. Progress in digital wireless communications resulted in extended use of mobile internet access, digital radios, automated highways and factories. However, with the increasing use of wireless services, the requirements on resources like battery power and radio spectrum are put under severe pressure. Therefore, the development of radio platforms that optimize the utilization of energy in addition to guaranteeing spectral efficiency becomes of great importance. Temporally and spectrally localized transmission strategies that minimize the energy spent to transmit the information-bearing symbols will be crucial towards achieving high energy efficiency [1].

The theory of wavelets offers many advantages for the design of wireless communications. The main property of wavelets for these applications is their ability to characterize signals with adaptive time-frequency resolution [2]. In this work, we do not pursue a multiresolution representation of a signal as in classical wavelet analysis. We rather consider the time-frequency representations called frames which are applied at a single resolution level [3] (page 53). Specifically, we present the development of wavelets that offer an exact representation of single-frequency and multi-frequency communications. Then, we provide an approach to wavelet optimization that minimizes the power to transmit the signal. Directions to the design of finite band wavelets are discussed.

INTRODUCTION

Solution Summary. The key idea is to represent the desired long-wavelength signal as superposition of compactly supported short pulses (referred to as wavelets or basis functions) that are shifted with an overlap with respect to one another and are radiated in a predetermined sequence by an array of small antennas [4]. The possibility of such a representation is facilitated by the results from Shannon's sampling theory, Fourier analysis, and the theory of analytic functions. The wavelets that enable the representation (referred to as signal fragmentation) can be optimized for minimum power use and shaped to allow for the radiation of the desired band of frequencies. In other words, our goal is to develop a small antenna system that emits prudently chosen signal fragments so that a required bandwidth of signals may be produced for AM, FM, FSK, and even covert communications, radar imaging/surveillance, ground perimeter surveillance, satellite communications, and many other applications.

Basic concept. The basic concept of this approach is to synthesize a desired far field signal as a combination of judiciously chosen pulses (basis functions or wavelets), as suggested in Figure 1. The technical approach involves obtaining the optimal compactly supported basis functions (wavelets) using the methods of sampling theory specially adopted for antenna synthesis, with the purpose of accurate signal reproduction in the far field using least power to produce the desired waveform. Thus, there are two fundamental goals: accuracy and efficiency. Figure 2 shows how the basis functions are modulated and combined.

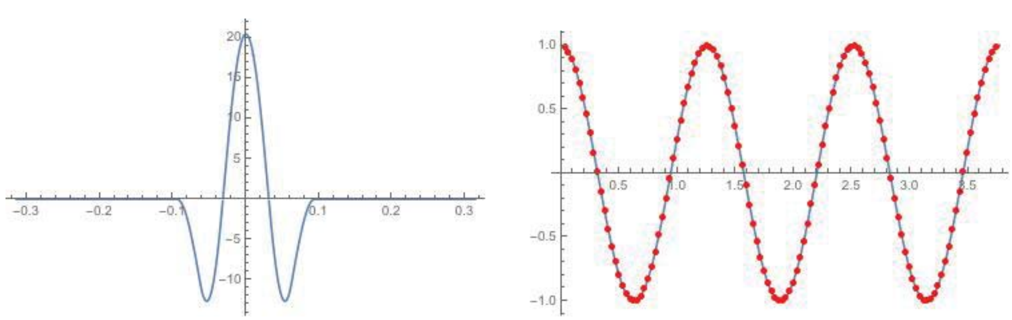

(a) Example of wavelet (b) Reconstruction by fragmentation

FIGURE 1. The desired signal of a given frequency constructed from basis functions of short duration

Application of Mathematics in Technical and Natural Sciences
AIP Conf. Proc. 2953, 080002-1–080002-7; https://doi.org/10.1063/5.0177458
Published by AIP Publishing. 978-0-7354-4720-2/$30.00

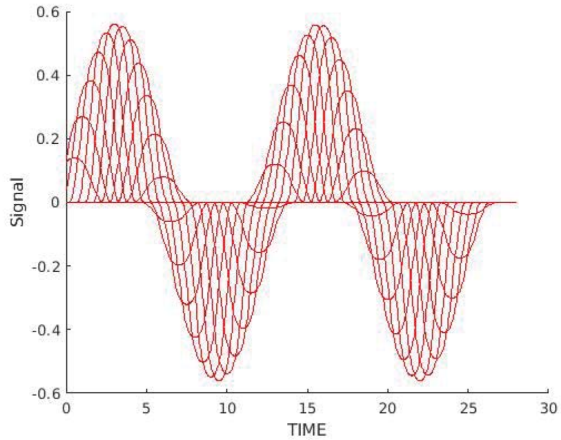

FIGURE 2. Formation of signal by individual wavelets. Since only a small number of wavelets overlap, individual antennas in an array can be used repeatedly: the proposed antenna system radiates like a Gatling gun fires bullets: each single antenna at a time with some overlap

BASIS FUNCTION MATHEMATICS

The fundamental concept of wavelets is that the propagating signal is decomposed into fragments.

Exact fragmentation for a sinusoidal wave

In this section, we present some results from [5, 6] that have served as the starting point for our subsequent analysis, in particular, the power optimization in the single-frequency and multi-frequency case.

Let ω_c be the desired carrier frequency and $G(t) = G_0 \sin \omega_c t$ be the radiated field of the antenna in its Fraunhofer zone. Then, for a simple "differentiator" antenna the required driving current is $I(t) = I_0 \cos \omega_c t$, where $I_0 = -G_0/\omega_c$. We will seek the following representation of the sinusoidal current $I(t) = I_0 \cos \omega_c t$:

$$I(t) = \sum_{n=-\infty}^{\infty} I(t_n) U(t - t_n). \tag{1}$$

The function $U = U(t)$ in (1) is the elementary pulse, or wavelet, that we assume compactly supported on the interval $[-\tau, \tau]$, i.e., $U(t) = 0$ for $t > \tau$. Hereafter, we will be interested in the case of short pulses compared to the period of the carrier oscillation: $\tau \ll \frac{2\pi}{\omega_c}$. The centers of individual wavelets in the sum (1) are shifted with respect to one another by equal increments $\sigma > 0$:

$$t_n = \sigma n, \quad n = 0, \pm 1, \pm 2, \pm 3, \ldots \tag{2}$$

Differentiation both sides of (1) yields:

$$I'(t) = G(t) = G_0 \sin \omega_c t = \sum_{n=-\infty}^{\infty} I(t_n) U'(t - t_n). \tag{3}$$

Formula (3) shows that the driving current $I(t)$ obtained by fragmentation (1)–(2) is guaranteed to generate the target CW signal $G(t) = G_0 \sin \omega_c t$ in the far field even though the radiated wavelets $U'(t - t_n)$ are not, generally speaking, the same as the original wavelets $U(t - t_n)$ at the antenna. The advantage of applying the fragmentation to the driving current $I(t)$ (as opposed to the radiated signal $G(t)$) is the automatic elimination of the direct current (DC) in the far field. Indeed, even if $U(t)$ has a DC component, which if $\tilde{U}(0) \neq 0$, the derivative $U'(t)$ does not. This is important because on one hand, direct current may not be radiated into the far field, but on the other hand, as our subsequent analysis shows, the wavelets U with desired properties often have a DC component.

The wavelet $U(t)$ is not specified yet. Its key desired property is that it should enable the exact reconstruction of the sinusoidal wave as per (1)–(2). Exactness implies that there will be no out-of-band frequencies, i.e., no spectral leakage. The following theorem can be obtained using the sampling theory. Hereafter, a tilde above a character denotes the Fourier transform, *e.g.*, $\tilde{U}(\omega) \equiv F[U](\omega)$.

Theorem 1. *Let $U = U(t)$ be compactly supported on $[-\tau, \tau]$: $U(t) = 0$ for $|t| > \tau$, and let $U \in L_2(\mathbb{R})$. Let also $\tilde{U}(\frac{2\pi n}{\sigma} \pm \omega_c) = 0$, $n = \pm 1, \pm 2$, and $\tilde{U}(\pm\omega_c) = A \neq 0$, where ω_c and σ are fixed and $0 < \tau \leqslant \sigma$. Then, $\tau = \sigma$ and the function $U(t)$ is determined uniquely (up to a multiplicative constant):*

$$\begin{aligned} \tilde{U}(\omega) &= \frac{A}{\operatorname{sinc}(\omega_c \sigma)} \operatorname{sinc}\left((\omega - \omega_c)\frac{\sigma}{2}\right) \operatorname{sinc}\left((\omega + \omega_c)\frac{\sigma}{2}\right), \\ U(t) &= \begin{cases} \frac{A}{\operatorname{sinc}(\omega_c \sigma)} \frac{1}{\sigma^2 \omega_c} \sin(\omega_c(\sigma - |t|)), & |t| \leqslant \sigma, \\ 0, & \text{otherwise.} \end{cases} \end{aligned} \tag{4}$$

The minimum compact support for the desired wavelet $U(t)$ is $[-\sigma, \sigma]$. Then, according to (4) we have:

$$U(t) \equiv U_{\min}(t) = \begin{cases} \frac{1}{\sin(\omega_c \sigma)} \sin(\omega_c(\sigma - |t|)), & |t| \leqslant \sigma, \\ 0, & \text{otherwise.} \end{cases} \tag{5}$$

No more than two consecutive wavelets $U_{\min}$ may overlap in (1) at any given moment of time. An example of $U_{\min}(t)$ is shown in Figure 3(a).

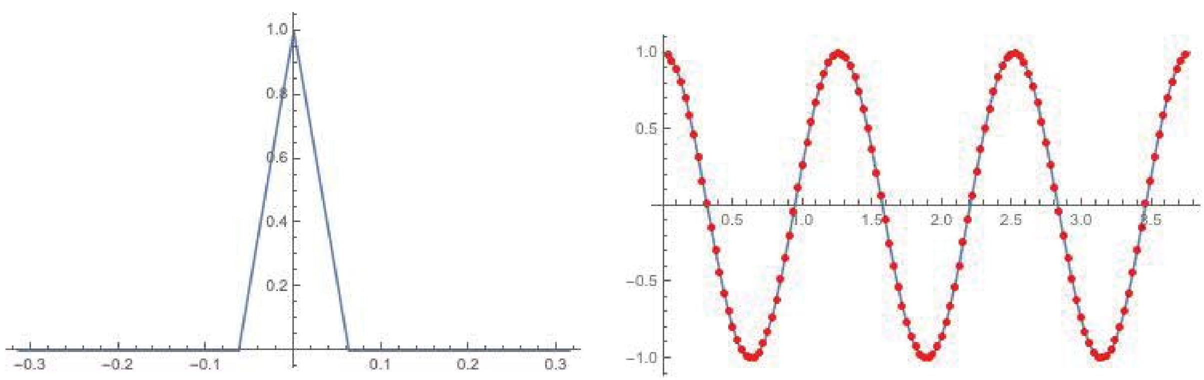

(a) Minimum support wavelet, equation (5)

(b) Reconstruction, defined by equation (1)

FIGURE 3. Left panel: minimum support wavelet (5) for $\omega_c = 5$ and $\sigma = 2\pi/100$. Right panel: reconstruction of $I(t) = \cos\omega_c t$, $\omega_c = 5$, over three full periods by means of formula (1) with a wavelet from the family (5)-(6). Red dots — fragmentation, blue curve — original time-harmonic signal

The central result that provides foundation for the subsequent optimization is given by the following

Corollary 2. *A family of admissible wavelets that guarantee no spectral leakage is given by*

$$U(t) = [W * U_{\min}](t), \tag{6}$$

where $U_{\min}$ is defined by (5) and $W \in L_2(\mathbb{R})$ can be any even compactly supported function of t, $t \in [-\alpha, \alpha]$, that additionally satisfies

$$\tilde{W}(\omega_c) = \tilde{W}(-\omega_c) = 1. \tag{7}$$

Note that, if $W(t)$ is sufficiently smooth, then the wavelet $U(t)$ given by (6) is also sufficiently smooth.

WAVELET POWER OPTIMIZATION

The power is given by the square integral of the elementary current U:

$$P = \int_{-\tau}^{\tau} [W * U_{\min}]^2(t)dt = 2\int_{0}^{\tau} U^2(t)dt = 2\int_{0}^{\tau} \left(\sum_{k=0}^{K} c_k b_k(t)\right)^2 dt. \tag{8}$$

In formula (8), $\tau = \alpha + \sigma$ and $b_k(t) = [W^{(k)} * U_{\min}](t)$, where $W^{(k)}$, $k = 0, 1, \dots, K$, are the basis functions chosen to represent $W(t)$ on its interval of support $[-\alpha, \alpha]$. In our implementation, we have used Chebyshev polynomials. For convenience, we can introduce the matrix $\boldsymbol{B}$ of dimension $(K+1) \times (K+1)$:

$$\boldsymbol{B} = \begin{bmatrix} b_{00} & b_{01} & \dots & b_{0,K} \\ b_{10} & b_{11} & \dots & b_{1,K} \\ \vdots & \vdots & \ddots & \vdots \\ b_{K,0} & b_{K,1} & \dots & b_{K,K} \end{bmatrix}, \quad \text{where} \quad b_{i,j} = \int_{0}^{\tau} b_i(t) b_j(t) dt. \tag{9}$$

Then, the expression (8) for power becomes:

$$P = 2\boldsymbol{c}^T \boldsymbol{B}\boldsymbol{c}, \quad \text{where} \quad \boldsymbol{c} = [c_0, c_1, \dots, c_K]^T. \tag{10}$$

As (10) and (8) are equivalent, the matrix $\boldsymbol{B}$ of (9) is SPD. In practice, the entries of the matrix $\boldsymbol{B}$ are evaluated by numerical quadratures.

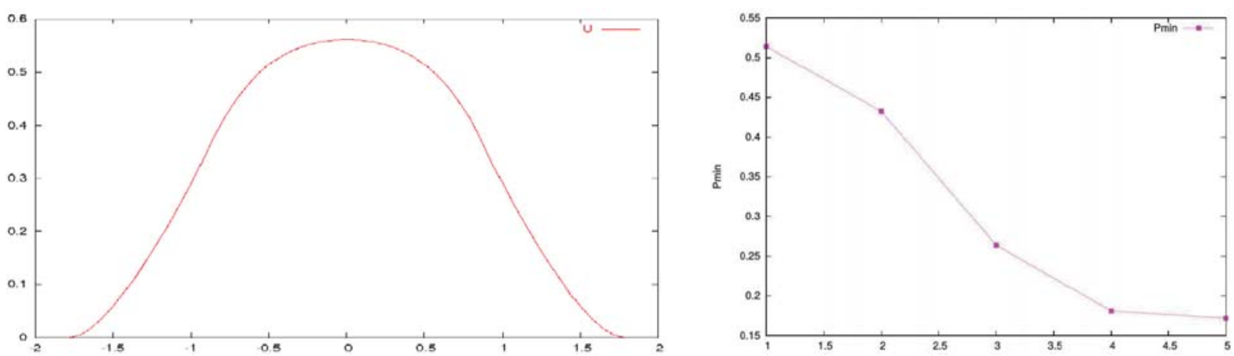

(a) Power minimized wavelet (6)

(b) The dependence of minimum power $P_{\min}$ on α

FIGURE 4. Examples of power minimization

The problem of minimizing P given by (8) subject to the constraints (7) has been solved numerically using two different approaches. The first one involved an expansion of $W(t)$ using RBFs with subsequent application of the Levenberg-Marquardt optimization. The second one employed a Chebyshev expansion of $W(t)$ plus Lagrange multipliers. The results from the two optimizations techniques matched one another with high precision. In Figure 4(a), we are showing an example of a power optimized wavelet given by formula (6) subject to constraint (7).

Of particular interest is the question of what happens to the minimum power $P_{\min}(\alpha)$ when α increases. Numerical observations indicate that $P_{\min}(\alpha)$ decreases as α grows, albeit with a slowing rate, see Figure 4(b). An intuitive argument that accounts for these observations is as follows.

MULTI FREQUENCY WAVELETS

Two distinct frequencies

Next, we develop wavelets that would guarantee the exact reconstruction of signals composed of a finite number of distinct frequencies. As our first example, let us consider a signal composed of two distinct frequencies $\omega_c^{(1)}$ and $\omega_c^{(2)}$:

$$I(t) = I_1 \cos \omega_c^{(1)} t + I_2 \cos \omega_c^{(2)} t. \tag{11}$$

For example, amplitude modulation (AM) of the carrier oscillation $\cos \omega_c t$ by a (much) lower frequency ω_m:

$$I_{AM}(t) = \cos \omega_m t \cos \omega_c t = \frac{1}{2}[\cos((\omega_c + \omega_m)t) + \cos((\omega_c - \omega_m)t)], \tag{12}$$

falls into the category of signals (11). Indeed, on the right-hand side of equation (12), we have two distinct frequencies: $\omega_c^{(1)} = \omega_c + \omega_m$ and $\omega_c^{(2)} = \omega_c - \omega_m$. We would like to build a wavelet $U(t)$ that enables the leakage-free reconstruction of the signal (11) by means of formula (1). Both τ and σ must be much shorter than the smaller of the two periods, $\frac{2\pi}{\omega_c^{(1)}}$ or $\frac{2\pi}{\omega_c^{(2)}}$.

Similar to formula (6), the wavelets that guarantee the exact representation of the dual-frequency signal (11) can be represented as

$$U(t) = [W * [U_{\min}^{(1)} * U_{\min}^{(2)}]](t), \tag{13}$$

where $U_{\min}^{(1)}(t)$ and $U_{\min}^{(2)}(t)$ are the minimum wavelets (5) that correspond to the frequencies $\omega_c^{(1)}$ and $\omega_c^{(2)}$, respectively. As $\operatorname{diam}\big(\operatorname{supp}[U_{\min}^{(1)} * U_{\min}^{(2)}]\big) = 4\sigma$, for $\operatorname{supp} U = [-\tau, \tau]$ we have $\tau = \alpha + 2\sigma$.

A finite number of distinct frequencies

The approach described in previous Section extends to a larger number of distinct frequencies:

$$I(t) = I_1 \cos \omega_c^{(1)} t + I_2 \cos \omega_c^{(2)} t + \ldots + I_N \cos \omega_c^{(M)} t. \tag{14}$$

Following the same rationale as in previous section, we obtain the desired wavelet in the time domain:

$$U(t) = [W * U_{\min}^{(1)} * U_{\min}^{(2)} * \ldots * U_{\min}^{(M)}](t). \tag{15}$$

Multi-frequency wavelet optimization

The dual-frequency wavelet (13) can be optimized to carry minimal power. We considered the case where $\alpha = 3.5 \times 10^{-9}$, $\sigma = 1.57 \times 10^{-9}$, $\omega_c^{(1)} = 1.00 \times 10^9$, and $\omega_c^{(2)} = 1.01 \times 10^9$. Let

$$W(t) = \sum_{k=0}^{K} c_k T_k \left(\frac{t}{\alpha} \right).$$

Figure 5 shows the double convolution product

$$[W * U_{\min}^{(1)} * U_{\min}^{(2)}](t)$$

that minimizes the power defined similar to (8) for Chebyshev degrees $K = 6$ and $K = 8$.

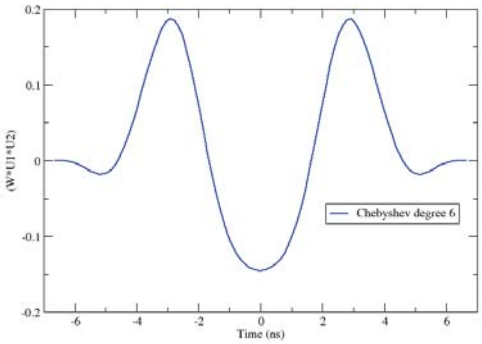

(a) Wavelets for $K = 6$

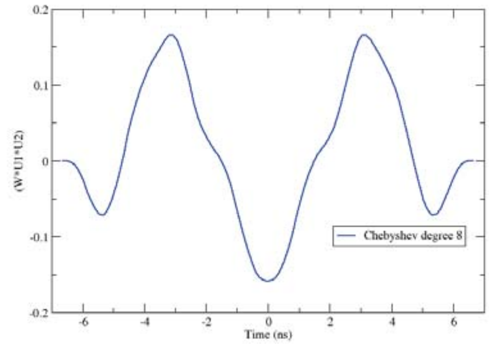

(b) Wavelets for $K = 8$

FIGURE 5. Optimized dual-frequency wavelets $[W * U^{(1)}_{\min} * U^{(2)}_{\min}](t)$

The results for three distinct frequencies. We considered the case where $\alpha = 3 \times 10^{-9}$, $\sigma = 1 \times 10^{-9}$, $\omega_c^{(1)} = 0.6 \times 10^9$, and $\omega_c^{(2)} = 0.75 \times 10^9$. $\omega_c^{(3)} = 0.9 \times 10^9$. Let

$$W(t) = \sum_{k=0}^{K} c_k T_k \left(\frac{t}{\alpha} \right).$$

Figure 6 shows the triple convolution product

$$[W * U^{(1)}_{\min} * U^{(2)}_{\min} * U^{(3)}_{\min}](t)$$

that minimizes the power defined similar to (8) for the Chebyshev expansions with $K = 4$ and $K = 6$.

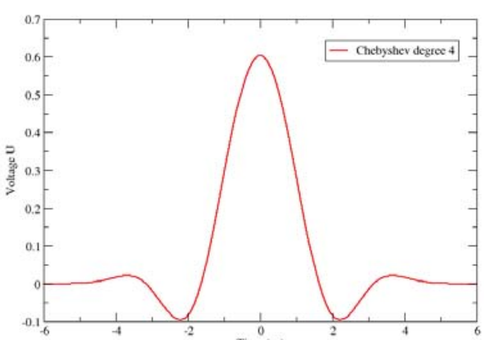

(a) Wavelets for $K = 4$

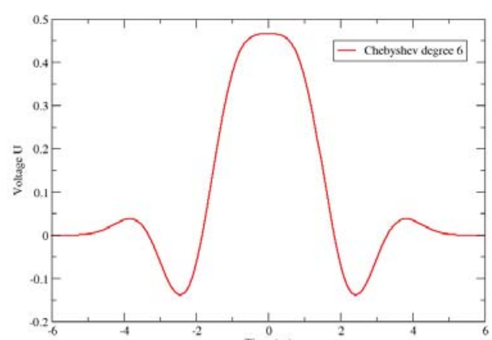

(b) Wavelets for $K = 6$

FIGURE 6. Optimized triple-frequency wavelets $[W * U^{(1)}_{\min} * U^{(2)}_{\min} * U^{(3)}_{\min}](t)$

Performance of a single-frequency wavelet for other frequencies

Let $I_2(t) = I_{2,0}\cos\omega_2 t$, where $\omega_2 \neq \omega_c$. We will use the minimum wavelet $U(t) = U_{\min}(t)$ of (5) designed for the frequency ω_c to reconstruct the current $I_2(t)$ by means of the fragmentation expansion (1):

$$I_{2,\text{rec}}(t) = \sum_{n=-\infty}^{\infty} I_2(t_n)U(t-t_n). \tag{16}$$

As $\omega_2 \neq \omega_c$, we expect that the reconstructed current $I_{2,\text{rec}}(t)$ of (16) will not coincide exactly with the original current $I_2(t)$. The is to estimate the corresponding reconstruction error. Our detailed estimation shows that for $\omega_2 < \omega_c$ and $\omega_c\sigma \ll 1$ we have

$$\max|I_2(t) - I_{2,\text{rec}}(t)| \leqslant I_{2,0}\omega_c^2\sigma^2\left(\frac{1}{6}+\frac{2}{\pi^2}\right).$$

or

$$\max|I_2(t) - I_{2,\text{rec}}(t)| \leqslant \text{const}\cdot(\omega_c\sigma)^2.$$

Consequently, the overall error of reconstruction (16) when the target frequency ω_2 is not equal to the design frequency ω_c, $\omega_2 < \omega_c$, decays quadratically with the small parameter $\omega_c\sigma$.

CONCLUSIONS

We presented families of wavelets that offer an exact leakage-free representation of single-frequency and multi-frequency signals. We have also developed an approach to minimize the power of the wavelets and assessed the performance of a single-frequency wavelet for the frequencies other than its design carrier frequency.

ACKNOWLEDGMENT

The work was supported by the US Army Research Office under contract number W911NF-20-C-0011. The content of the paper does not necessarily represent the position or policy of the US Government.

REFERENCES

1. H. Nikookar, *Wavelet Radio: Adaptive and Reconfigurable Wireless Systems Based on Wavelets* (Cambridge University Press, Cambridge, UK, 2013).
2. M.K. Lakshmanan and H. Nikookar, A review of wavelets for digital wireless communication, Springer Journal on Wireless Personal Communication **37**(3-4), 387–420 (2006).
3. I. Daubechies, “Ten lectures on wavelets,” Society for Industrial and Applied Mathematics (SIAM), Philadelphia, PA, 1992.
4. R. Albanese, *Private Communication*, 2018.
5. R. Caflisch, H. Hsu Chou, and J. W. Siegel, Accuracy, Efficiency and Optimization of Signal Fragmentation, Multiscale Model. Simul. **18**(2), 737–757 (2020).
6. R. E. Caflisch, H. H. Chou, and J. W. Siegel, Efficient frame projection of amplitude-modulated signals, CAM Report 18-45, University of California, Los Angeles, CA, October 2018.